INTERNATIONAL JOURNAL OF
COASTAL, OFFSHORE & ENVIRONMENTAL ENGINEERING IJCOE Vol.10/No. 4/ Autumn 2025 (28-34)

Available online at: www. Ijcoe.org

Characteristics of a Circular Cylinder Response under Vortex-Induced Vibration in a Subcritical Flow Regime

Mohammadreza Vaselali[1], Maryam Soyuf Jahromi[2*], Abolfazl Pourrajabian[3]

[1]Ph.D Student in Physical Oceanography, Department of Nonliving Resources of Atmosphere and Ocean, Faculty of Marine Science and Technology, University of Hormozgan, Bandar Abbas, Iran, vaselali.mr@gmail.com
[2] Associate Professor of Physical Oceanography, Department of Nonliving Resources of Atmosphere and Ocean, Faculty of Marine Science and Technology, University of Hormozgan, Bandar Abbas, Iran, soyufjahromi@hormozgan.ac.ir*
[3] Associate Professor, Department of Energy, Materials and Energy Research Center (MERC), Karaj, Iran, a.pourrajabian@merc.ac.ir

ARTICLE INFO

Article History:
Received : 18 May 2025
Accepted : 14 Jan 2026

Keywords:
Vortex-induced vibration
VIV
Turbulence model
Lift coefficient
Drag coefficient

ABSTRACT

In this study, the characteristics of vortex-induced vibration (VIV) of a rigid, smooth circular cylinder elastically mounted in the water flow are investigated. The cylinder has one degree of freedom and is constrained to oscillate only in the vertical direction. The flow Reynolds number lies within the Transition of Shear Layer 3 (TrSL3) region of the subcritical flow regime. The governing equations, namely the continuity and Navier-Stokes equations, are solved using computational fluid dynamics (CFD). The finite volume method is employed for discretizing the equations, implemented through the ANSYS Fluent software. The Pressure Based solver and the PISO algorithm are utilized to couple the equations. The two-dimensional unsteady Reynolds-averaged Navier-Stokes (URANS) equations are solved using the k-ω SST turbulence model. A simplified mathematical model describes the system dynamics and fluid forces associated with the cylinder's vortex-induced vibration. Examination of the vortices shed in the wake region reveals a P+S vortex shedding pattern. Additionally, the time history of the cylinder's displacement ratio exhibits a sinusoidal shape, whereas the recorded lift and drag coefficient data are non-sinusoidal due to the P+S vortex shedding mode. Frequency analysis of the cylinder's response indicates that the oscillation frequency of the cylinder matches the dominant frequency of the lift force. Furthermore, the dominant frequency of the drag force is twice that of the lift one.

1. Introduction

In engineering research, investigating flow behavior around bluff bodies and the fluid-structure interaction (FSI) effects is of paramount importance. The interaction between a bluff body and a fluid flow, depending on the Reynolds number, can lead to various flow regimes and consequently, flow separation in the wake region, resulting in the formation of vortices. At low Reynolds numbers, flow separation does not occur but as the Reynolds number increases, the flow separation gradually initiates, leading to flow instability and the onset of a phenomenon known as vortex shedding with a characteristic frequency. Consequently, the wake region takes the shape of a vortex street. The periodic shedding of vortices induces fluctuating pressure and hydrodynamic forces on the body. The component of this force perpendicular to the flow direction has a frequency similar to the vortex shedding frequency, while the frequency of the component parallel to the flow is twice the vortex shedding frequency [1,2,3]. If the body is free to move, these forces induce oscillatory motion, known as vortex-induced vibration (VIV) [1]. This phenomenon has numerous applications in civil and marine structures. Of particular interest is its use in renewable energy harvesting devices [4].

In this regard, extensive research has been conducted to advance the knowledge in this field and find the key parameters that factor in. The strong dependence of VIV on the Reynolds number has driven numerous research studies to focus on this aspect [5,6,7]. Studies carried out in recent decades have employed a variety of methods including experimental investigations [5,8] as well as numerical simulations [1,9].

While numerous studies have investigated vortex-induced vibration (VIV) of circular cylinders, predominantly at lower Reynolds numbers or through experimental methods [1,5,8], this research distinguishes itself by employing a two-dimensional computational fluid dynamics (CFD) approach with the k-ω SST turbulence model to examine the characteristics of vortex-induced vibration of a single-degree-of-freedom circular cylinder in the TrSL3 region of the subcritical flow regime, as classified by Zdravkovich [10]. This investigation provides novel insights into the P+S vortex shedding mode, characterized by alternating pair and single vortices, which results in non-sinusoidal lift and drag coefficients, a less commonly reported feature in prior numerical analyses. These findings enhance the understanding of fluid-structure interactions in the TrSL3 regime and underscore the efficacy of two-dimensional URANS simulations in capturing complex VIV phenomena at higher Reynolds numbers. Furthermore, recent reviews [11,12] underscore the need to explore such vortex shedding patterns at higher Reynolds numbers, making this work a distinct contribution to understanding fluid-structure interaction in this challenging flow regime.

2. Materials and Methods

2.1. Physical Model

Figure 1 illustrates the schematic of the physical model. This model comprises a rigid, smooth circular cylinder with a diameter D and mass m, elastically mounted in the fluid flow using two linear springs with a stiffness coefficient K. The damping coefficient c represents structural damping, arising from internal friction and applied to the model. The cylinder is mounted horizontally in a cross-flow and constrained to oscillate only in the y-direction.

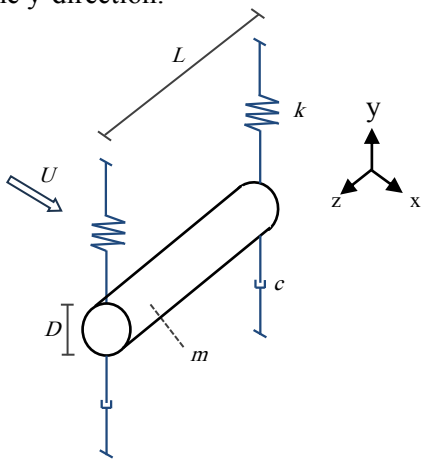

Figure 1. Schematic of the physical model: An elastically mounted circular cylinder with linear spring and damper exposed to a cross-flow.

The water flow is uniform, steady, and directed in the x-direction. Table 1 presents the parameters of the physical model and fluid properties. The system mass includes the effective mass of the spring and the mass of the oscillating cylinder. The Reynolds number of the flow, calculated based on the cylinder diameter D, is 1.25×10^5 which indicates a subcritical flow regime. A characteristic of this regime is a fully turbulent boundary layer and a turbulent wake region.

Table 1. Physical model and the media parameters

Parameter	Symbol	Unit	Value
Cylinder diameter	D	m	0.125
Cylinder length	L	m	0.9144
Total oscillating mass	m_{osc}	kg	12.7
Total system elasticity (stiffness)	K	N/m	1025
System damping	c_{system}	Ns/m	18.5
System natural frequency in water	$f_{n,water}$	Hz	1.04
Fluid dynamic viscosity	μ	Ns/m^2	0.001003
Fluid density	ρ	kg/m^3	998.2
Nondimensional mass, mass ratio	m^*	-	1.12

2.2 Governing Fluid Flow Equations and Turbulence Model

The governing fluid flow equations are the continuity and Navier-Stokes equations. These equations were solved using computational fluid dynamics (CFD). The finite volume method was employed to discretize the equations, implemented through the ANSYS Fluent software. The Pressure Based solver and the PISO algorithm were utilized to couple the equations. The k-ω SST turbulence model was employed to solve the unsteady Reynolds-averaged Navier-Stokes (URANS) equations.

2.3 Mathematical Model

A simplified mathematical model describes the system dynamics and fluid forces associated with the vortex-induced vibration of the cylinder. The motion of the cylinder in the y-direction, perpendicular to both the flow direction and the cylinder's axis, is modeled by a second-order linear equation, as described in Eq. (1).

$$m_{osc}\ddot{y} + c_{system}\dot{y} + K_{spring}y = F_{fluid,y} \quad (1)$$

where y represents the cylinder displacement, m_{osc} is the mass of the oscillating system which includes one third of the spring mass, K_{spring} is the spring stiffness, c_{system} is the system damping coefficient, and $F_{fluid,y}$ is the force exerted by the fluid on the body in the y-direction. Due to the periodic nature of vortex shedding, the pressure on the cylinder surface also undergoes periodic fluctuations. Consequently, there are periodic variations in the forces applied to the cylinder surface. The force resulting from the pressure

distribution can be divided into two components: one perpendicular to the flow (the lift force, F_L) and the other parallel to the flow (the drag force, F_D). The lift force emerges when vortex shedding initiates and oscillates at the same frequency as the vortex shedding. Concurrently, the drag force also oscillates similarly to the lift force. It should be noted that the drag force, in addition to its fluctuating component, also has a constant component that arises from friction and pressure difference.

3. Results

Figure 2 shows the vortices formed in the wake region, which appear as a single vortex on one side of the vortex street and a pair of vortices on the other side. After the cylinder's transient response, the vortex shedding pattern is such that in one half-period of the cylinder's oscillation, a single vortex forms and sheds, while in the next half-period, two vortices shed into the wake.

The displacement ratio time history (Figure 3, up) demonstrates that the cylinder undergoes oscillatory motion perpendicular to the flow due to periodic forces induced by vortex shedding. The maximum amplitude of cylinder oscillation obtained in this study is 0.086 m, and the maximum non-dimensional oscillation amplitude (ratio of oscillation amplitude to cylinder diameter) is 0.69. These values were determined after the stabilization of cylinder oscillation and following the transient response. According to the calculations, the root mean square value of the nondimensional displacement ($y^*_{R.M.S.}$) is 0.46. Furthermore, this oscillatory motion has a frequency of 1.1 Hz. Figure 3 (down) depicts the FFT analysis of displacement ratio.

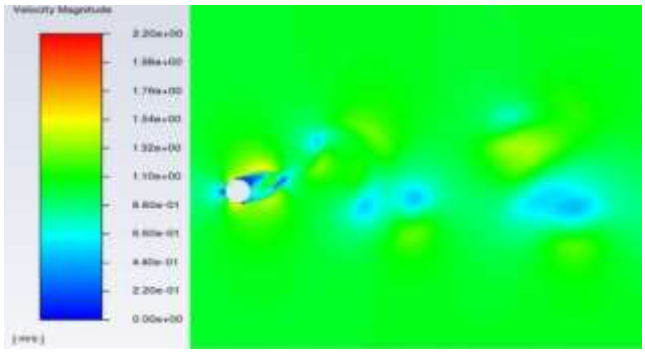

Figure 2. Vortex shedding behind the cylinder according to the velocity magnitude

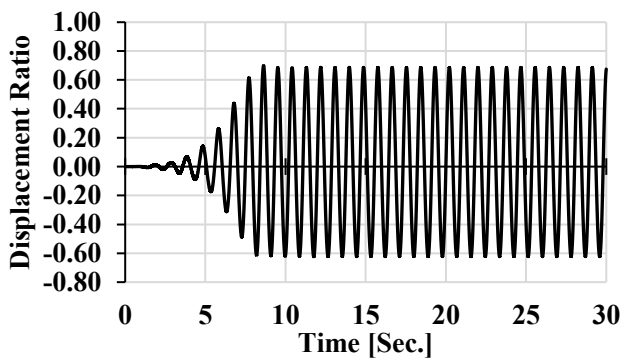

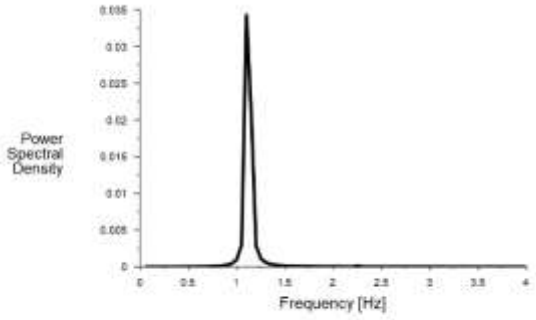

Figure 3. (Up) Time history and (down) frequency spectrum of the cylinder displacement ratio

As mentioned, periodic vortex shedding generates an oscillating lift force, inducing the transverse oscillatory motion of the cylinder. Figure 4 (up) shows time records of the lift coefficient. The maximum value of the lift coefficient after the stabilization of cylinder oscillation is 0.93, and the minimum value is -0.56. Moreover, its time-average value is 0.06. Based on the calculations, the R.M.S. value of the lift coefficient ($C_{l,R.M.S.}$) is 0.44. The FFT analysis indicates that the predominant frequency of the oscillating lift coefficient is 1.1 Hz, with additional frequency components at 2.25 Hz and 3.35 Hz (Figure 4, down).

The maximum value of the drag coefficient after the stabilization of cylinder oscillation is 2.89, and its time-average value is 2.09. Furthermore, the dominant frequency of the drag force, according to the FFT analysis, is 2.25 Hz. The time history of the drag coefficient and its components frequencies are shown in Figure 5.

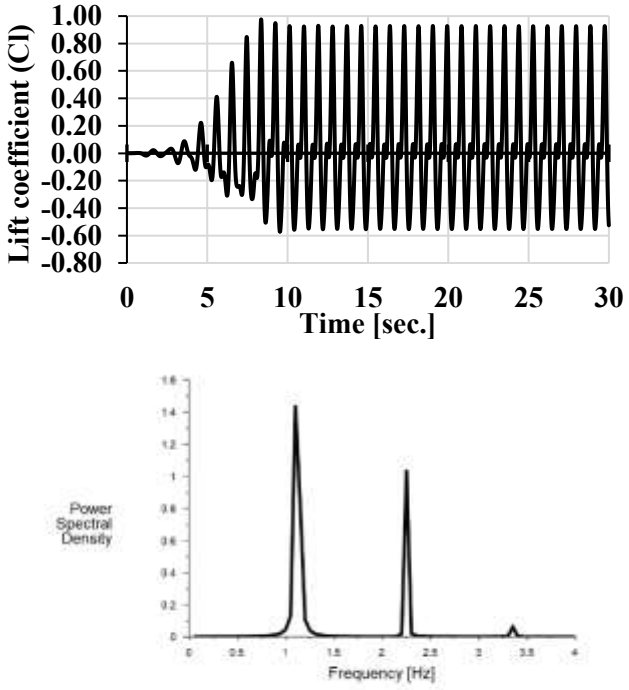

Figure 4. (up) Time records of the lift coefficient and (down) its frequency spectrum

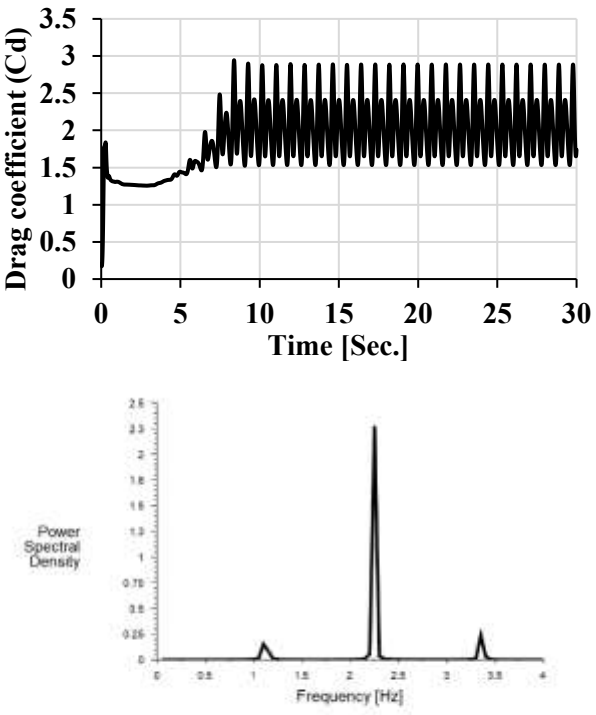

Figure 5. (up) Time records of the drag coefficient and (down) its frequency spectrum

4. Discussion

The Reynolds number of 1.25×10^5 corresponds to a subcritical flow regime. In this regime, the boundary layer transitions from laminar to turbulent, and the wake region is also turbulent. The shedding vortices in the subcritical regime, exhibit a high degree of organization, as evident in Figure 2. Due to the oscillatory motion of the cylinder in the fluid, different wake structures can be created downstream of the flow. These structures are influenced by various factors such as the Reynolds number, cylinder surface roughness, cylinder end conditions, length-to-diameter ratio of the cylinder, and structural characteristics. As observed in Figure 2, in each oscillation period of the cylinder, a pair of vortices is shed on one side of the Kármán Street and a single vortex on the other side, corresponding to the P+S mode.

After the transient response of the cylinder, the displacement ratio time history exhibits a sinusoidal shape, bounded by a value of 0.7. A compilation of data of the displacement ratio from other researchers is presented in Table 2. To interpret the discrepancies in the cylinder response, understanding the characteristics of the flow regime and the near-wake region is crucial.

Table 2. Vortex induced vibration displacement ratio data

Investigators	Reynolds number	m*ζ	A/D
Sahu et al. [13]	50000	N.A	0.51
Abbaspour et al. [9]	80000	N.A	0.62
Vikestad et al. [14]	14000-65000	0.012	1.13
Present experiments	125000	0.066	0.69
Raghavan [15]	8000-150000	0.251	1.97
Ding et al. [16]	70000-250000	N.A	2.0
Sahu et al. [13]	150000	N.A	0.75
Sahu et al. [13]	300000	N.A	0.39

Figure 6 illustrates the phase difference between the displacement ratio of the cylinder and the lift coefficient. The presence of a phase difference between the cylinder displacement and the lift force indicates a time delay in the structural response to the applied forces. The lift coefficient time history (Figure 4, up) does not exhibit a sinusoidal pattern and displays two peaks in each half-period of cylinder oscillation. The values of these two peaks differ significantly, with the smaller peak being less than 0.1. Consequently, the lift coefficient remains near zero for an extended duration. The non-sinusoidal nature of the lift coefficient arises from the vortex shedding pattern in the wake. The vortex shedding, in accordance with a specific pattern and interactions between shed vortices, generates multiple oscillatory components within the lift force, each characterized by distinct frequency, phase, and amplitude. Figure 4 (down) illustrates the power spectral density of the lift coefficient. The frequencies of components with lower power are approximately 2 and 3 times the dominant frequency. The dominant frequency of the lift coefficient is 1.1 Hz, which coincides with the frequency of the cylinder oscillation. The non-zero time-averaged lift coefficient, resulting from the difference between its maximum and minimum magnitudes, indicates an asymmetry in the time-series data of the lift coefficient. This asymmetry in the positive and negative amplitudes of cylinder motion stems from the wake structure and the presence of the P+S mode in vortex shedding. In other words, the alternation in the number of vortices shed in successive half-periods of cylinder oscillation results in unequal pressure forces being applied to the cylinder in the positive and negative amplitudes of oscillation. The positive values of the lift coefficient are bounded by a value of 1, and the negative values by -0.6.

Table 3 compares the C_l with results reported by other researchers in the subcritical flow regime. In this regime, the boundary layer transitions from laminar to turbulent. This transition influences the vortex shedding frequency, vortex strength, and, consequently, the lift forces. It can be observed that the lift coefficient increases with increasing Reynolds number. Figure 7, presented by Norberg [17], also illustrates $C_{l,\,R.M.S}$ versus Re. The results of the present study align with this figure.

Table 3. Vortex induced vibration Maximum and R.M.S. lift coefficient data

Investigators	Reynolds number	$C_{l,max}$	$C_{l,R.M.S.}$
Khalak and Williamson [18]	1700	-	0.03
Khalak and Williamson [18]	9750	-	0.25
Khalak and Williamson [18]	12500	-	0.29
Abbaspour et al. [9]	80000	0.80	-
Present experiments	125000	0.93	0.44
Sahu et al. [13]	150000	-	1.25

The rapid increase in the drag coefficient at the beginning of the its time history diagram (Figure 5, up) is attributed to the development of the initial flow and the formation of the boundary layer. After the transition from initial conditions, leading to the development of a stable wake behind the cylinder, periodic fluctuations in the drag coefficient occur, which is a characteristic of VIV and a consequence of the periodic shedding of vortices from the cylinder surface.

The drag force, like the lift one, is composed of several oscillatory components with different frequencies, caused by vortex shedding from the cylinder surface. As a result, the drag coefficient exhibits a non-sinusoidal oscillation, as shown in Figure 5 (up). The periodic part of the drag coefficient time history is bounded by the values of 1.5 and 2.9. Frequency analysis of the drag coefficient (Figure 5, down) reveals that the dominant frequency is 2.25 Hz, with contributions from other significant components at 1.1 and 3.35 Hz.

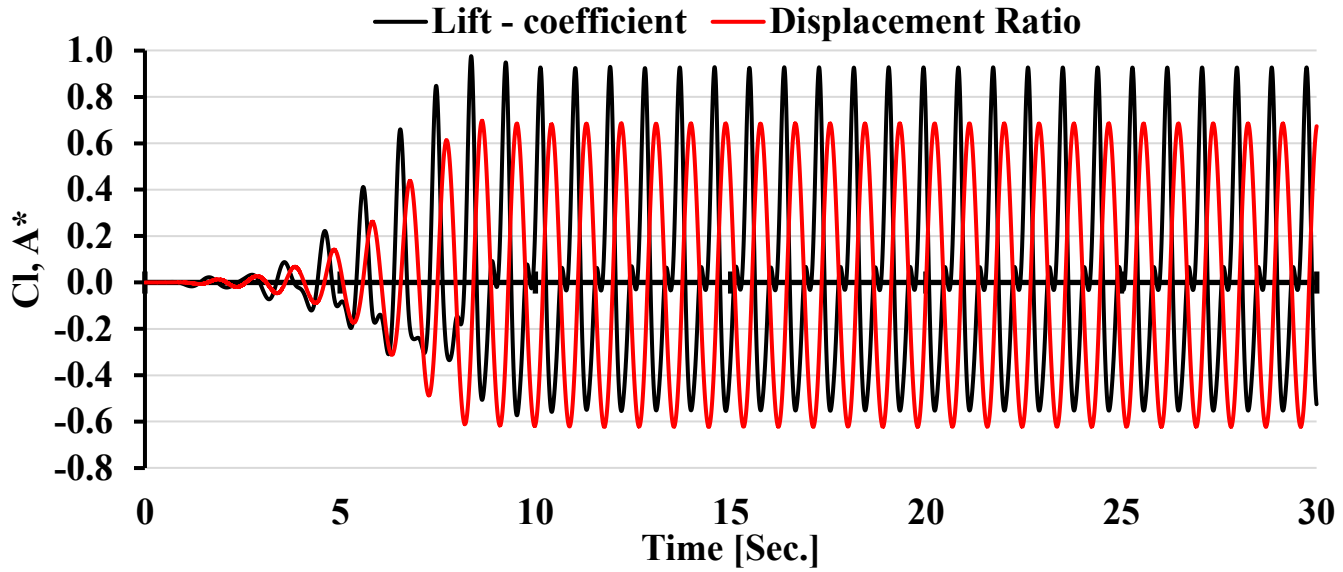

Figure 6. Time records of the lift coefficient and displacement ratio

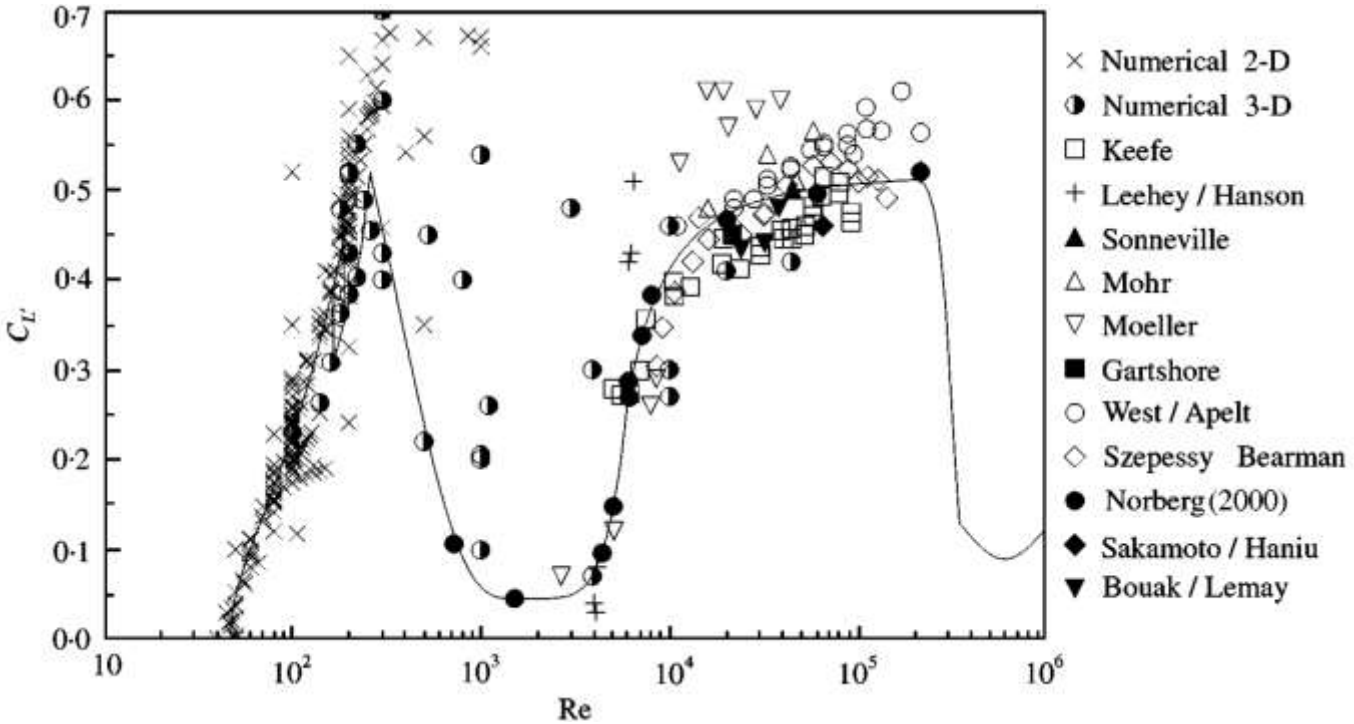

Figure 7. Fluctuating lift coefficient plotted versus Reynolds number [Reproduced from Norberg (2000)]

The drag coefficient oscillates at roughly double the frequency of the lift coefficient. This is because the lift force requires a full cycle of vortex shedding from both sides of the cylinder to complete its oscillation. In contrast, the drag force undergoes a full oscillation cycle with vortex shedding from each side of the cylinder [19]. Table 4 presents the mean drag coefficient (C_d) values at the end of the subcritical regime. With increasing Reynolds number and approaching the critical regime, the drag coefficient decreases. This is due to the elongation of the vortex formation region [10]. The high value of the drag coefficient results in increased energy dissipation within the fluid-structure system, influencing the amplitude of cylinder oscillation. Consequently, the displacement ratio of the cylinder (Table 2) in the present study is lower than that reported by Sahu et al. [13].

Table 4. Vortex induced vibration mean drag coefficient data

Investigators	Reynolds number	$\overline{C_d}$
Present study	125000	2.09
Sahu et al. [13]	150000	0.95

5. Conclusions

Simulation of the single degree of freedom vortex-induced vibration (VIV) of a rigid circular cylinder elastically mounted was implemented by solving unsteady Reynolds-averaged Navier-Stokes equations using the k-ω SST turbulence model in the Transition of Shear Layer 3 (TrSL3) region of the subcritical flow regime. The following results were obtained and discussed. First of all, the vortices shed in the wake were well-organized. The vortex shedding pattern was shown in one period of cylinder oscillation. In this regard, P+S vortex pattern mode was observed. Second, the cylinder exhibited a sinusoidal oscillatory motion perpendicular to the flow direction, driven by the periodic forces induced by vortex shedding. Oscillatory motion occurs at the same frequency as the dominant frequency of lift force fluctuations, but with a time lag caused by structural delays in responding to the applied force. In the presence of the P+S vortex shedding mode, the time histories of the lift and drag forces exhibited non-sinusoidal behavior. Instead, they were composed of the superposition of multiple oscillatory components with varying frequencies and amplitudes. FFT analysis of the lift and drag coefficients revealed the dominant frequency as well as other frequencies. According to this analysis, the dominant frequency of the drag coefficient was twice that of the lift coefficient. And finally, compared to previous studies, it was observed that a larger drag coefficient was associated with a smaller amplitude of oscillation. This is attributed to the fact that higher drag coefficients result in greater energy dissipation from the system, which in turn affects the displacement of the cylinder.

6. Acknowledgment

The authors express profound gratitude to Dr. Narges Amrollahi Biuki, associate professor of University of Hormozgan, for her exceptional contributions to this work.

7. References

1. Williamson, C.H.K., & Govardhan, R., (2004). Vortex-induced vibrations. Annu Rev Fluid Mech 36, 413–455. https://doi.org/10.1146/annurev.fluid.36.050802.122128.
2. Sarpkaya, T., (2004). A critical review of the intrinsic nature of vortex-induced vibrations, Journal of Fluids and Structures, 19(4), 389–447. https://doi.org/10.1016/j.jfluidstructs.2004.02.005
3. Zhang, J., & Tang, Y., (2022). Numerical study on vortex-induced vibration of a circular cylinder near a plane boundary at low Reynolds numbers, Applied Ocean Research, 119, 103028. https://doi.org/10.1016/j.apor.2021.10302
4. Hafizh, M., Muthalif, A.G.A., Renno, J., Paurobally, M.R., Bahadur, I., Ouakad, H., Sultan Mohamed Ali, M., (2022). Vortex induced vibration energy harvesting using magnetically coupled broadband circular-array piezoelectric patch: Modelling, parametric study, and experiments, Energy Conversion and Management, 276 (2023) 116559**.** https://doi.org/10.1016/j.enconman.2022.116559
5. Raghavan, K, & Bernitsas, M.M., (2011). Experimental investigation of Reynolds number effect on vortex induced vibration of rigid circular cylinder on elastic supports., Ocean Eng 38(5–6), 719–731. https://doi.org/10.1016/j.oceaneng.2010.09.003
6. Martins, F.A.C., Avila, J.P.J., (2019). Effects of the Reynolds number and structural damping on vortex-induced vibrations of elastically-mounted rigid cylinder, International Journal of Mechanical Sciences, Volume 156, June 2019, Pages 235-249. https://doi.org/10.1016/j.ijmecsci.2019.03.024
7. Gu, J., Fernandes, A.C., Han, X., Kuang, X., Chen, W., (2022). Numerical investigation of Reynolds number effects on vortex-induced vibrations at low and moderate Re regimes, Ocean Engineering, Volume 245, 1 February 2022, 110535. https://doi.org/10.1016/j.oceaneng.2022.110535
8. Narendran, K., Murali, K., & Sundar, V., (2014). Vortex-induced vibrations of elastically mounted circular cylinder at Re of the O (10^5), J Fluids Struct 54:503–521. https://doi.org/10.1016/j.jfluidstructs.2014.12.006

9. Abbaspour, M., Nematikourabbasloo, N., & Mohtat, P., (2022). Numerical simulation of vortex-induced vibration of a smooth circular cylinder at the subcritical regime, Proceedings of the Institution of Mechanical Engineers, Part M: Journal of Engineering for the Maritime Environment. 236(4), 916-937. https://doi.org/10.1177/14750902221088
10. Zdravkovich, M. M., (1990). Conceptual Overview of Laminar and Turbulent Flows Past Smooth and Rough Circular-Cylinders, Journal of Wind Engineering and Industrial Aerodynamics, 33(1-2), 53-62. https://doi.org/10.1016/0167-6105(90)90020-D
11. Hong, K. S., Shah, U. H., (2018). Vortex-induced vibrations and control of marine risers: A review. Ocean Engineering, 152, 300–315. https://doi.org/10.1016/j.oceaneng.2018.01.086.
12. Zhao, M., (2023). A review of recent studies on the control of vortex-induced vibration of circular cylinders. Ocean Engineering, 285(Part 2), 115389. https://doi.org/10.1016/j.oceaneng.2023.115389.
13. Sahu, T.R., Chopra, G., & Mittal, S., (2021). Vortex-Induced Vibration of a Circular Cylinder at High Reynolds Number, In: Braza, M., Hoarau, Y., Zhou, Y., Lucey, A.D., Huang, L., Stavroulakis, G.E. (eds) Fluid-Structure-Sound Interactions and Control, FSSIC 2019. Lecture Notes in Mechanical Engineering. Springer, Singapore. https://doi.org/10.1007/978-981-33-4960-5_30
14. Vikestad, K., Vandiver, J. K., & Larsen, C. M., (2000). Added Mass and Oscillation Frequency for a Circular Cylinder Subjected to Vortex-Induced Vibrations and External Disturbance, Journal of Fluids and Structures, 14(7), 1071-1088. https://doi.org/10.1006/jfls.2000.0308
15. Raghavan K., (2007). *Energy Extraction from a Steady Flow Using Vortex Induced Vibration*, Ph.D. thesis, University of Michigan.
16. Ding, J., Balasubramanian, S., Lokken, R., & Yung, T., (2004). *Lift and Damping Characteristics of Bare and Staked Cylinders at Riser Scale Reynolds Numbers*, [Paper presentation]. Proceedings of Offshore Technology Conference, Houston, Texas, May 2004, Paper No. 16341. https://doi.org/10.4043/16341-MS
17. Norberg, C., (2000). Flow around a Circular Cylinder: Aspects of Fluctuating Lift, Journal of Fluids and Structures, 15(3-4), 459-469. https://doi.org/10.1006/jfls.2000.0367
18. Khalak, A., & Williamson, C. H. K., (1999). Motions, Forces and Mode Transitions in Vortex-Induced Vibrations at Low Mass-Damping, Journal of Fluids and Structures, 13(7-8), 813-851. https://doi.org/10.1006/jfls.1999.0236
19. Rafati Zarkak, M., Barati, E., & Abolfazli Esfahani J., (2019). Numerical Study of Energy Harvesting of Vortex Induced Vibration Phenomenon of Circular Cylinder with Various Sectors at Low Reynolds Number, Modares Mechanical Engineering. 19(7), 1687-169. DOR: 20.1001.1.10275940.1398.19.7.6.2